TNO report
PML 1998-A106

Evaluation of the ballistic resistance of composite materials under FSP impact: experimental results

TNO Prins Maurits Laboratory

Lange Kleiweg 137
P.O. Box 45
2280 AA Rijswijk
The Netherlands

Phone +31 15 284 28 42
Fax +31 15 284 39 59

Date
March 1999

Author(s)
M.J. Deutekom

Classification		
Classified by	:	P. van der Geijs
Classification date	:	20 January 1999
		(This classification will not change)
Title	:	Ongerubriceerd
Managementuittreksel	:	Ongerubriceerd
Abstract	:	Ongerubriceerd
Report text	:	Ongerubriceerd
Annexes A - C	:	Ongerubriceerd

Copy no.	:	12	
No. of copies	:	25	
No. of pages	:	39	(incl. annexes, excl. RDP & distribution list)
No. of annexes	:	3	

All information which is classified according to Dutch regulations shall be treated by the recipient in the same way as classified information of corresponding value in his own country. No part of this information will be disclosed to any party.

The classification designation Ongerubriceerd is equivalent to Unclassified.

TNO Prins Maurits Laboratory is part of
TNO Defence Research which further consists of:

TNO Physics and Electronics Laboratory
TNO Human Factors Research Institute

Netherlands Organization for
Applied Scientific Research (TNO)

Managementuittreksel

Titel	:	Evaluation of the ballistic resistance of composite materials under FSP impact: experimental results
Auteur(s)	:	Ir. M.J. Deutekom
Datum	:	maart 1999
Opdrachtnr.	:	A96KL453
Rapportnr.	:	PML 1998-A106

In het kader van het onderzoek naar de ballistische bescherming van personeel wordt in opdracht van LBBKL-KPU-bedrijf in een Canadees-Nederlandse samenwerking het gedrag van composiet materialen bij een inslag van een FSP (Fragment Simulerend Projectiel) onderzocht (A96KL453). Het onderzoek wordt uitgevoerd door het TNO Prins Maurits Laboratorium (TNO-PML), Divisie Wapens en Wapenplatformen, researchgroep Munitie-uitwerking en Ballistische Bescherming (MB) en het Defense Research Establishment Valcartier (DREV), Canada. Om de uitwisseling van gegevens te vergemakkelijken is in overleg met KPU afgesproken dat dit rapport in de engelse taal wordt geschreven.
Het doel van dit project is inzicht te krijgen in de wisselwerking tussen projectiel en lichtgewicht composiet materialen tijdens inslag van het projectiel. Dit inzicht wordt verkregen door het uitvoeren van geïnstrumenteerde ballistische inslagexperimenten op composietplaten in combinatie met numerieke simulaties hiervan.
De researchgroep MB verricht op het Laboratorium voor Ballistisch Onderzoek (LBO) geïnstrumenteerde ballistische inslag experimenten. De resultaten van deze experimenten worden gebruikt ter validatie van de software, die wordt ontwikkeld door de University of British Columbia (UBC) in Vancouver in opdracht van DREV. De software, die DREV aan MB levert, bestaat uit een analytisch computer model genaamd IMPACT en een composiet faalmodel als subroutine voor het eindige elementen programma LSDYNA (2D-versie). Om de toepasbaarheid van de beide modellen te kunnen valideren, moeten meerdere composietmaterialen getest worden. Daarom is door DREV in samenwerking met de groep MB een test matrix opgesteld. Er zijn inslag experimenten met standaard FSP's (1,1 g en 2,8 g) op Kevlar vezel versterkte composieten (KFRP) uitgevoerd. En er zijn inslagexperimenten met konische FSP's (120° en 37° hele tophoek) op glasvezelversterkte composieten (GFRP) uitgevoerd. Voor alle experimenten zijn de inslagsnelheden rond de V_{50} waarde genomen. De opzet en de resultaten van deze experimenten worden in dit rapport beschreven.

Het wisselwerkingsmechanisme tussen projectiel en doelplaat is een proces wat plaatsvindt binnen een tijdsduur van enkele tientallen microseconden. Dit mechanisme is in beeld gebracht door het gebruik van twee diagnostische

apparaten: de hoge snelheid röntgen camera (IMAX) en de laser interferometer (VISAR).
Met de IMAX wordt de contour van de doorbuiging van de achterzijde van de composietplaat en de positie van het projectiel tijdens het impact proces op acht discrete punten gemeten. Gedurende het penetratieproces is het met de röntgenstralen van de IMAX mogelijk om het projectiel zichtbaar te maken, terwijl het in het doorgebogen gedeelte van het composiet zit.
Met de VISAR wordt gedurende het penetratieproces de snelheid van de achterzijde van de composietplaat op één plaats gemeten. De meetplaats komt overeen met de schootslijn van het projectiel en dus het penetratiekanaal van het projectiel. Door het snelheidsprofiel te intergreren wordt de verplaatsing van de achterzijde van de composietdoelplaten verkregen. Door beide meettechnieken tegelijk te gebruiken, wordt een onderling vergelijk mogelijk en daarmee een grote nauwkeurigheid van het verloop van de doorbuiging van de doelplaat.

De experimenten op de KFRP panelen zijn succesvol verlopen en gaven zeer bruikbare data voor het verifieren van de computersimulaties. De doorbuigingsprofielen verkregen met de IMAX en de VISAR kwamen in bijna alle experimenten zeer goed met elkaar overeen.
De resultaten tonen de volgende trend voor het penetratieproces van een FSP op een aramidevezelversterkt plastic. In het begin van het proces falen de vezels op afschuiving en wordt het nog intacte deel door de FSP vooruit geduwd, waardoor deze vezels op rek worden belast. In deze fase wordt de kinetische energie van het projectiel geabsorbeerd door het afschuivingsproces en door de rekenergie in de vezels. Als het projectiel het composiet geheel penetreert, is dit de enige fase van het penetratieproces. Als het projectiel door het composiet wordt gestopt, is er een tweede fase waarin het afschuivingsproces is opgehouden. Dit gebeurt zodra de snelheid voldoende is afgenomen. De nog intact zijnde vezellagen worden dan verder vooruit geduwd en zetten daardoor de resterende kinetische energie van het projectiel om in rekenergie.

De experimenten op de GFRP panelen waren alleen succesvol voor de stompe (120°) FSP's. Echter de laterale dimensies van de GFRP panelen waren dusdanig klein dat in al deze experimenten het delaminatiegebied de zijkanten bereikte. Deze experimenten zijn daardoor niet representatief voor een groot paneel waarbij de delaminatie niet tot de zijkanten komt.
De experimenten op de GFRP panelen met de scherpe (37°) FSP's waren onbruikbaar, omdat dit projectiel van richting veranderde terwijl het het doelmateriaal penetreerde. Hierdoor komt het penetratiekanaal niet meer overeen met de schootslijn. Dit werd hoogstwaarschijnlijk veroorzaakt doordat het projectiel niet spingestabileerd was en een scherpe punt had. Het projectiel krijgt bij inslag gemakkelijk een asymmetrische belasting, die niet gecorrigeerd kan worden. Een spingestabileerd projectiel kan zo'n belasting vaak grotendeels wel corrigeren. Door de asymmetrische belasting wijkt het projectiel tijdens het penetreren van zijn rechte baan af. De data met het scherpe projectiel is hierdoor

niet bruikbaar voor de verificatie van het simulatiemodel, omdat daarin wordt aangenomen dat het projectiel het composiet in een rechte lijn penetreert.

Contents

1 Introduction

The personal equipment of the soldier includes protective clothing against ballistic threats. Personal protection equipment consists more and more of polymeric composite materials, because with these materials it is possible to reduce the weight without reducing the ballistic protection or to provide a higher level of protection for a given weight.
Up until now, the design of lightweight protective structures have been based primarily on experimental ballistic performance data. Understanding the deformation and failure mechanisms involved in the impact of composite targets is important in effectively designing a protection system to defeat a projectile. To achieve this design goal, it is necessary to have a reliable analysis tool that can deal with the details of material behaviour under impact events. Such a simulation program can be used to determine how the various properties of the target and the projectile parameters influence the target behaviour. However, it is always necessary to have reliable experimental data to calibrate and validate the simulation predictions.
The University of British Columbia (UBC) in Vancouver is developing an analytical simulation program called IMPACT [1] and a composite failure model for the LS DYNA hydrocode [2], both for ballistic impact on composite materials under assignment of the Defence Research Establishment Valcartier (DREV). Therefore a joint project with DREV was started to study the impact behaviour of polymeric composite materials. In this project, TNO Prins Maurits Laboratory (TNO-PML) performed instrumented ballistic impact experiments on two types of fibre reinforced plastics impacted by FSPs (Fragment Simulating Projectiles). This data can then be used to further develop and to validate the simulation programs. In exchange, TNO-PML will receive these programs.

Two types of diagnostic equipment were used for the instrumented ballistic impact experiments which TNO-PML performed: a cineradiographic high-speed camera (IMAX) and a Velocity Interference System for Any Reflector (VISAR). With the IMAX system, it is possible to measure the deformation of the composite as well as the position of the FSP during penetration. With the IMAX however, the deformation is measured at eight discrete times. With the VISAR system it is possible to measure the deformation of the rear face continuously.

Chapter 2 discusses the experimental set-up and the diagnostic equipment, i.e. IMAX and VISAR, in more detail. Chapter 3 shows the global results of all the experiments. The measured data is graphically shown in Annex C. Chapter 4 discusses the results in more detail. Conclusions are given in Chapter 5.

2 Experiments

To study the impact event of a rigid projectile and a composite plate, experiments have been performed at the Laboratory for Ballistics Research (LBO) at Ypenburg, which is part of TNO-PML, Division Weapons and Weapon Platforms, Munition Effects and Ballistic Protection Research Group (MB).
Figure 1 gives a schematic overview of the experimental set-up. Figure 2 gives a photographic picture of the set-up. The equipment shown in Figure 1 is (1a, b, c) the IMAX, (2) the VISAR, (3) lense and mirror for focusing the VISAR laser beam, (4) two light screens for projectile velocity measurement, and (5) the accelerator. The IMAX consists of three parts: an X-Ray gun (1a), an Image Converter tube (Thompson tube) (1b), and the IMACON high-speed camera (1c).

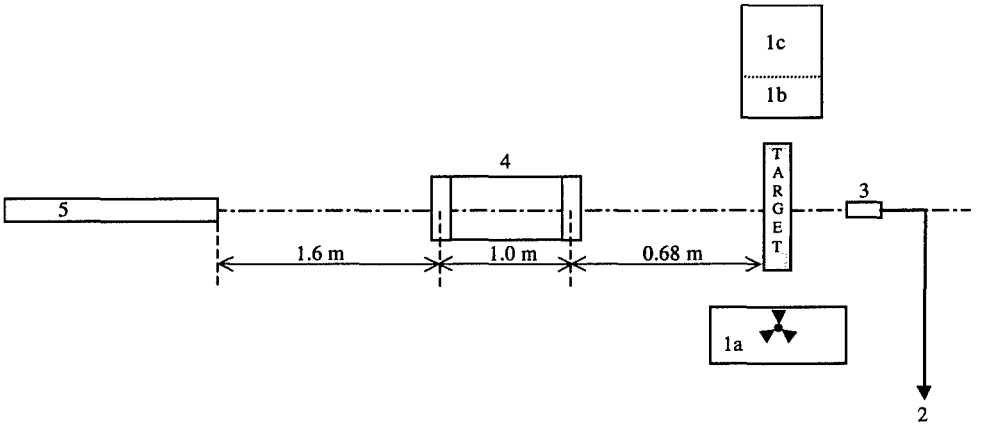

Figure 1: Schematic overview of the experimental set-up for the instrumented impact experiments.

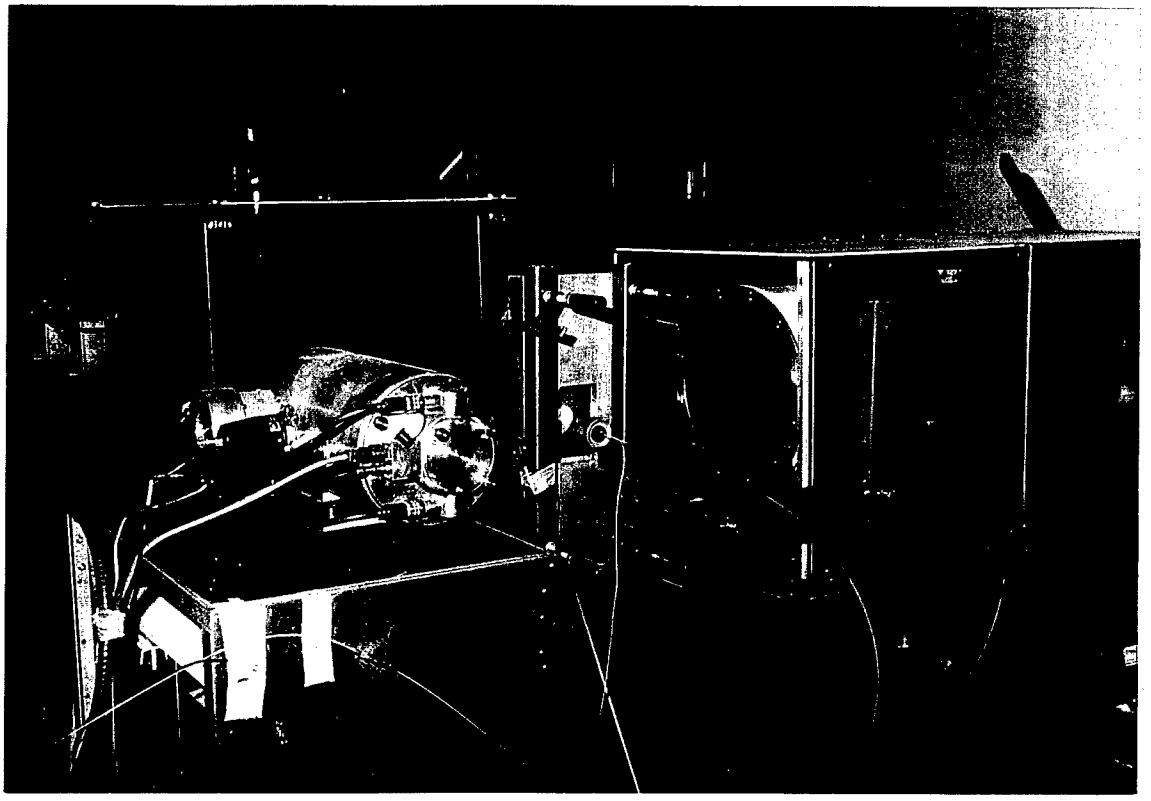

Figure 2.a: Photograph of the set-up seen from the rear side (980816-12a).

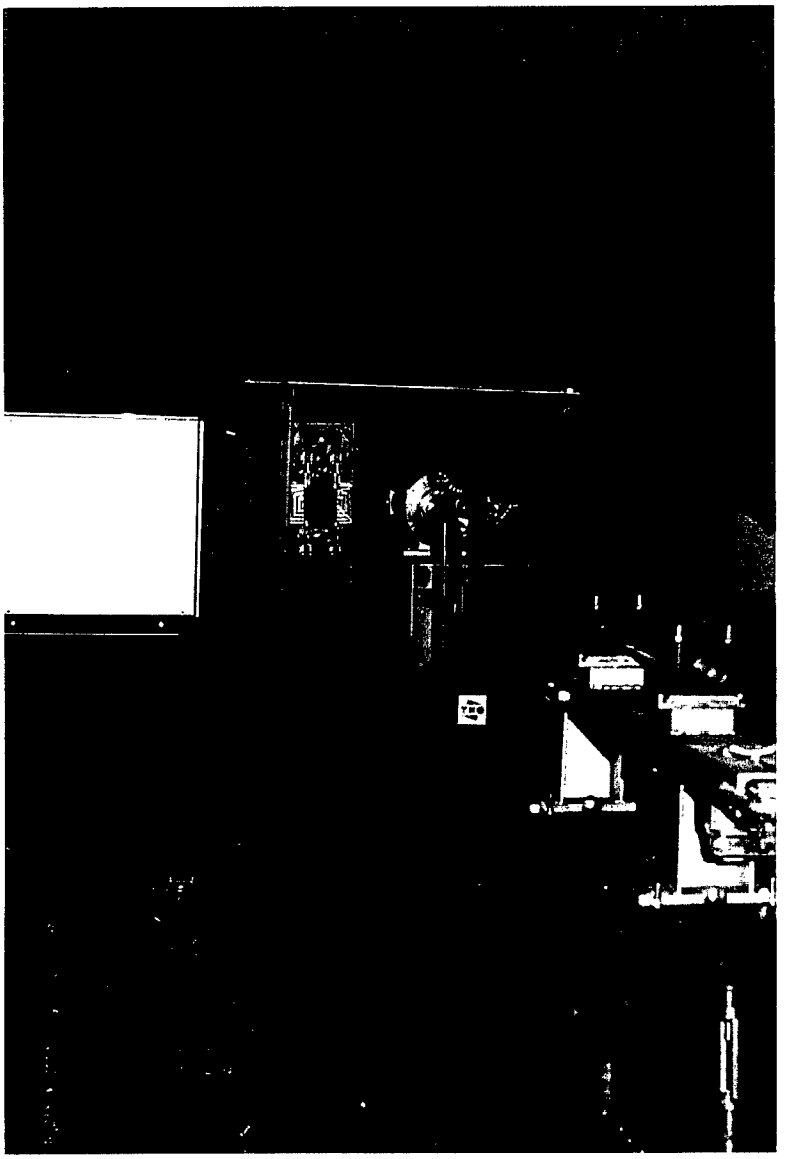

Figure 2.b: Photograph of the set-up seen from the front (980816-13A).

The diagnostic equipment used for studying the deformation of the backface of the composite targets as well as the motion of the projectile are the IMAX and the VISAR system. Section 2.1 gives a short description of these systems. Section 2.2 gives the experimental details such as which projectiles, target materials and the velocities used.

2.1 Equipment

IMAX

With the IMAX system it is possible to measure the deformation of the rear side of the composite target as well as the position of the FSP during penetration.
IMAX stands for IMAcon X-ray system. This system is able to make high-speed framing pictures with X-rays. The system consists of three parts as shown in Figure 1: an X-Ray gun (1a), an Image Converter tube (Thompson tube) (1b), and the IMACON high-speed camera (1c).
The X-ray tube is a specially designed X-ray gun, developed by X-Tek in the United Kingdom. It can operate from 70 to 150 kV, with different current settings. The speciality of the X-ray gun is that it can produce either single- or multiple-pulsed X-ray beams. The X-rays from the gun penetrate through the target into the image converter tube, which converts the X-rays into visible light. The IMACON camera, an electro optical camera, converts the light into electrons which are shifted and focused onto a phosphor screen. A polaroid film, placed against the phosphor screen, captures the frames. The IMAX system is capable of taking 8 pictures at a recording speed of 10,000 to 1 million frames per second.

VISAR

During the entire impact event the velocity of the back-face is measured with a VISAR. The VISAR is a laser Doppler interferometer which is able to measure velocity changes in time of any surface which gives a sufficient reflection. The VISAR uses an Argon Ion laser with a wavelength 514.5 μm, and a power of 2 Watt (single line). The laserlight is transmitted through a fibre (of 50 μm diameter) and a lens system which focuses the light on the back of the target. The reflected light is captured by the same lens system and is guided through an additional fibre (of 1000 μm diameter) into the VISAR.
If the surface is moving, the reflected light will have a Doppler shift. The VISAR measures the phase shift of the light by dividing the light into two legs, a reference leg and a delay leg, with a different path length. When these beams are combined, interference will occur. From this interference signal the velocity change as a function of time can be determined. By varying the length of the delay leg, the sensitivity of the VISAR can be adjusted. This length is referred to as the K-factor, which gives the velocity change of one fringe count during an acceleration. The interference signals are recorded by a digitizer. The signals from the digitizer are relayed to a PC and converted into the velocity signal by signal analysis software specially designed for the VISAR.

2.2 Experimental set-up

DREV has subcontracted two Canadian universities to assist in developing simulation models: The University of British Columbia (UBC) in Vancouver and

Carleton University in Ottawa. UBC has developed an analytical model for composite materials called IMPACT [1] and a failure model for composites for the hydrocode LS DYNA. Carleton University has been developing a helmet model for the hydrocode LS DYNA for their aramide helmet impact simulations. To validate their models and analytical simulation program, the universities suggested testing different materials and threats.

2.2.1 Target panels

Carleton University delivered aramid fibre reinforced plastic (KFRP) with a thickness of 10 mm and UBC delivered glass fibre reinforced plastic (GFRP) of two thicknesses, namely 12.7 mm and 19.0 mm. In order for the UBC to compare our results with theirs, we used the same support fixture, which is a standard support fixture for impact testing at Boeing. The drawing of the specimen holder is shown in Annex A. The areal dimensions of the specimens have to be adjusted to the fixture and are 52.4 mm by 101.6 mm for all specimens.

2.2.2 Projectiles

The KFRP panels are tested with standard 1.1 grams and 2.85 grams Fragment Simulating Projectiles (FSPs). The accelerator used for both FSPs is a smooth bore propellant powered accelerator. The FSP was accelerated full bore, without a sabot. The GFRP panels are tested with conical-nose cylindrical projectiles with two different tip cone angles, namely 37° and 120°. The projectiles are made up of 4140 steel with a hardness of 28 Rc. The nominal mass of these projectiles is 4.28 grams and their geometrical dimensions are shown in Annex B. The projectile diameter and skirt dimensions were chosen to provide a good fit with the TNO-PML's 308 calibre gun barrel, which is a smooth bore propellant powered accelerator.

2.2.3 Test Matrix

The ballistic impact experiments on the KFRP panels using standard 1.1 g and 2.8 g FSPs were performed at velocities below and above the V_{50}. The impact velocities (Vin) used are shown in Table 1. The impact velocity of 650 m/s and of 500 m/s are above the V_{50} for the 1.1 g FSP and the 2.8 FSP, respectively. In all the experiments, only 1 shot is fired in the centre of the target.

Table 1: Test matrix for the KFRP panels.

FSP projectile (g)	V_{in} (m/s)	Number of shots
1.1	500	1
1.1	550	2
1.1	600	2
1.1	650	1
2.8	350	1
2.8	400	2
2.8	450	2
2.8	500	1

The ballistic impact experiments on the GFRP panels using both conical-nosed projectiles were performed at velocities that span a narrow range around the ballistic limit velocity (V50). At these velocities it is assumed that the maximum amount of impact energy is dissipated into the target. The corresponding V_{50} velocities are shown in Table 2. Also in these experiments, only 1 shot is fired in the centre of the target.

Table 2: Test matrix for the GFRP panels.

Tip angle projectile (degree)	Thickness (mm)	Estimated V_{50} (m/s)	Number of shots around the V_{50}
37	12.7	320	5
37	19.0	422	5
120	12.7	525-554	5
120	19.0	730-860	5

3 Results

The experiments were performed with the experimetal set-up described in Chapter 2. The yaw before impact could be measured from the IMAX pictures. All the experiments showed no significant yaw (< 3°) of the projectile before impact. So no experiment had to be rejected, because of too much yaw.
The measured testing conditions of the experiments with the KFRP panels and the GFRP panels are respectively given in Table 3 and Table 4. For every experiment, the tables show the projectile used and the impact velocity measured with the two light-screens located before the target. Table 4 also shows the thickness of the target. Both show also if the IMAX and VISAR data could be collected succesfully. The frame speed of the IMAX pictures was changed between the experiments. Therefore the frame speed used for every experiment is also shown.

Table 3: Test conditions of experiments on the KFRP panels.

Exp. number	FSP type (g)	V_{in} (m/s)	IMAX Y/N[1]	IMAX frame speed (frames/second)	VISAR Y/N[1]
1	1.1	704	Y	2.5×10^4	N
2	1.1	588	Y	2.5×10^4	N
3	1.1	586	Y	2.5×10^4	Y
4	1.1	560	Y	2.5×10^4	Y
5	1.1	564	Y	2.5×10^4	N[2]
6	1.1	545	Y	2.5×10^4	Y
7	1.1	483	Y	2.5×10^4	Y
8	2.8	490	Y	2.5×10^4	N[2]
9	2.8	398	Y	2.5×10^4	Y
10	2.8	417	N	2.5×10^4	Y
11	2.8	386	Y	5×10^4	Y
12	2.8	446	Y	5×10^4	Y
13	2.8	461	Y	5×10^4	Y
14	2.8	321	Y	5×10^4	Y
15	2.8	511	Y	5×10^4	Y

1 Y: Yes; N: No.

2 VISAR data unusable, because VISAR measuring point not on maximum displacement.

Table 4: Test conditions of experiments on the GFRP panels.

Exp. number	Panel thickness (mm)	Tip angle projectile (degree)	V_{in} (m/s)	IMAX Y/N[1]	IMAX frame speed (frames/second)	VISAR Y/N[1]	Remarks
16	12.7	120	557	Y	5×10^4	Y	
17	12.7	120	517	Y	5×10^4	Y	
18	12.7	120	526	Y[3]	5×10^4	Y	
19	12.7	120	520	N	5×10^4	N	
20	12.7	120	548	Y[3]	5×10^4	Y	
21	19	120	778	Y[3]	5×10^4	Y	
22	19	120	785	Y	5×10^4	Y	
23	19	120	778	Y[3]	5×10^4	Y	
24	19	120	741	Y[3]	5×10^4	Y	
25	19	120	660	Y[3]	5×10^4	Y	
26	12.7	37	330	Y	5×10^4	N[2]	Unusable data[4]
27	12.7	37	278	Y	5×10^4	N[2]	Unusable data[4]
28	12.7	37	339	Y	5×10^4	N[2]	Unusable data[4]
29	12.7	37	347	Y	5×10^4	N[2]	Unusable data[4]
30	12.7	37	388	Y	5×10^4	Y	
31	12.7	37	339	Y	5×10^4	N[2]	Unusable data[4]
32	19	37	466	Y	5×10^4	Y	
33	19	37	413	N	5×10^4	N	
34	19	37	420	Y[3]	5×10^4	Y	
35	19	37	426	Y	5×10^4	N[2]	Unusable data[4]
36	19	37	450	Y	5×10^4	N[2]	Unusable data[4]

1 Y: Yes; N: No.

2 VISAR data unusable, because VISAR measuring point not on maximum displacement.

3 Projectile insufficiently visible on IMAX picture.

4 IMAX and VISAR data unusable, because the projectile deflected from its trajectory (i.e. the line of fire) within the target.

IMAX measurements

From the IMAX pictures, the displacement of the backface surface of the KFRP target and of the FSP can be measured from the frontface of the target. This is done with a magnifying glass (10 X).

Figure 3 shows the IMAX frame sequence of experiment 15, in which a 2.8 g FSP impacted a KFRP panel at 511 m/s. The figure also indicates the time and time-sequence of the frames. Time of impact is 0 μs. The projectile impacts the target from the right. In the first frame, the back of the projectile is still in front of the target. In the second frame, the back of the target starts to deform. From the third frame, the position of the projectile can be seen and measured.

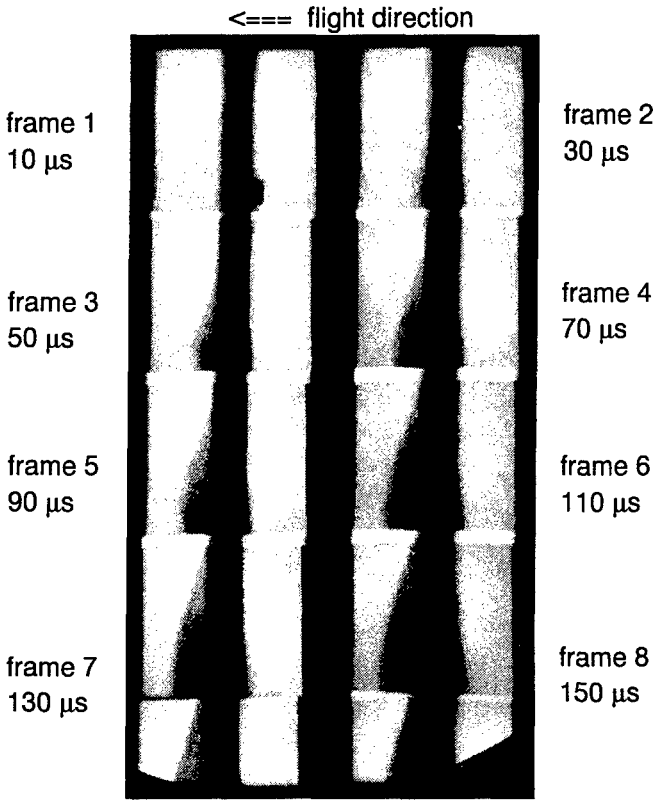

Figure 3: IMAX frame sequence experiment 15.

VISAR measurements

The velocity profile of the VISAR system is generated by counting the fringes from the digitised interference signal. The backface of the target accelerates within 0-20 µs after impact. Then the maximum velocity of the backface is reached and the backface starts to decelerate. It was not possible to determine the acceleration of the backface surface with the VISAR in any of the experiments, because the settings of the VISAR were not suitable for measuring fast velocity changes. So the fringes of the VISAR signal correspond mainly with the deceleration of the backface surface. The boundary condition for determining the initial velocity is the final velocity of the backface of the target, because it is zero after the last fringe appears. The time at which the velocity of the backface is zero can be verified with the IMAX data, because it corresponds with the time that the maximum defelection is reached.

From the velocity profile generated from the VISAR data, a curve fit is made. By integrating this function the displacement curve is obtained. From the IMAX data shown in Figure 3, it can be seen that at 10 µsec the displacement of the backface is zero and at 30 µsec it has already moved. Therefore, 10 µsec is taken for the offset value of the VISAR displacement curve.

The analysis of the VISAR data is more accurate than that of the IMAX data, once the boundary conditions for the initial displacement velocity and the displacement offset are chosen properly.

The data obtained from experiment 15 is graphically displayed in Figure 4. This figure shows the maximum displacement of the backface of the composite as a function of time measured at eight dicrete points with the IMAX and continuously with the VISAR. It also shows the displacement of the projectile measured from the IMAX frame sequence, and it shows the velocity of the backface of the target measured with the VISAR.
Figure 4 shows that the displacement of the backface measured with the IMAX and with the VISAR correspond well.

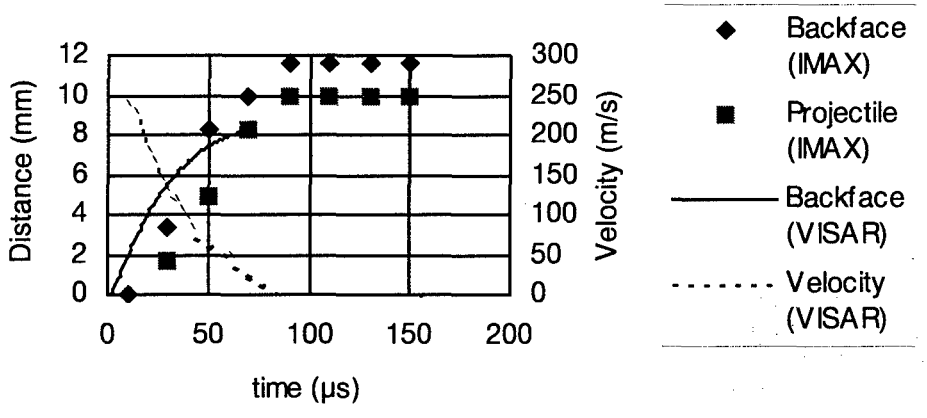

Figure 4: Displacement and velocity of the backface surface and displacement of the projectile as a function of time after impact (experiment 15).

In the same manner as described above, all the experiments are analysed and graphically derived and are shown in Annex C. The results are discussed in the next chapter.

4 Discussion

Chapter 3 gives the test conditions of the experiments. Table 3 in Chapter 3 shows that almost all the diagnostic results for the KFRP experiments were successful. The results of the KFRP experiments are discussed in more detail in Section 4.1. Table 4 in Chapter 3 shows that many of the experiments with the sharp nose (tip angle 37°) FSP impacting the GFRP panels gave unusable VISAR data, because the projectile deflected from its trajectory (i.e. the line of fire) within the target. For simulation purposes, the projectile is assumed to penetrate in a straight line. For this reason the IMAX data of these experiments (numbers 26 to 29, 31, 35 and 36) is not graphically displayed in Annex C. The results of the GFRP experiments are discussed in more detail in Section 4.2.

4.1 Experiments with the KFRP panels

The results of one experiment with the KFRP panels, experiment 15, is shown in Figures 3 and 4 in Chapter 3. The measured data of all the experiments with the KFRP panels are shown in Annex C. From these data the following remarks can be made:

- the backfaces of the targets reach their maximum velocity within the first 10 μsec. This velocity change could not be recorded with the VISAR, because the settings were not suitable for measuring such fast velocity changes;
- the displacement profile of the back was measured directly from the IMAX data and indirectly from the velocity profile of the VISAR by integrating the velocity profile. The two displacement profiles correspond well with each other, except for experiment number 5. The reason for this one exception is still unclear;
- the maximum displacement of the back was reached after 80 to 100 μsec after impact in all experiments, except for no. 8;
- in the first 10 experiments, in which the measuring time frame of the IMAX is 300 μsec, it could be seen that the maximum displacement of the backface of the target is not the same as the permanent indentation;
- after 30-80 μsec, the distance between the projectile and backface of the target will stay the same. In other words, after that time the projectile does not penetrating the target anymore, but pushes the intact part of the target in front of it.

The results of these experiments show the following trend for the penetration process of an FSP impacting a KFRP panel. First the FSP penetrates the fibre reinforced composite by shearing the fibres. In this phase, a part of the kinetic energy of the projectile is absorbed by the shearing process of the target. The FSP also pushes the intact material in front of it. This causes the fibres to stretch. So another part of the kinetic energy of the projectile is absorbed by strain energy in the fibres. After the shearing process is over, the straining of the fibres continues

until all the kinetic energy is absorbed or until the projectile has completely penetrated the target. A part of the energy absorbed by the fibres is elastic energy. That is probably the reason why, when the projectile is stopped, the displacement of the backface of the target decreases.

For these experiments it must be realised that the lateral dimensions of the target panels are rather small and there could be some boundary effects. For all the experiments, except experiment 15, the delamination area was within the boundary limits. For the experiment with the 2.8 g FSP at the highest velocty, experiment 15, the delamination area reached the boundaries. This can be seen clearly in Figure 5, which shows the post-impacted specimen of experiment 15 from the side.

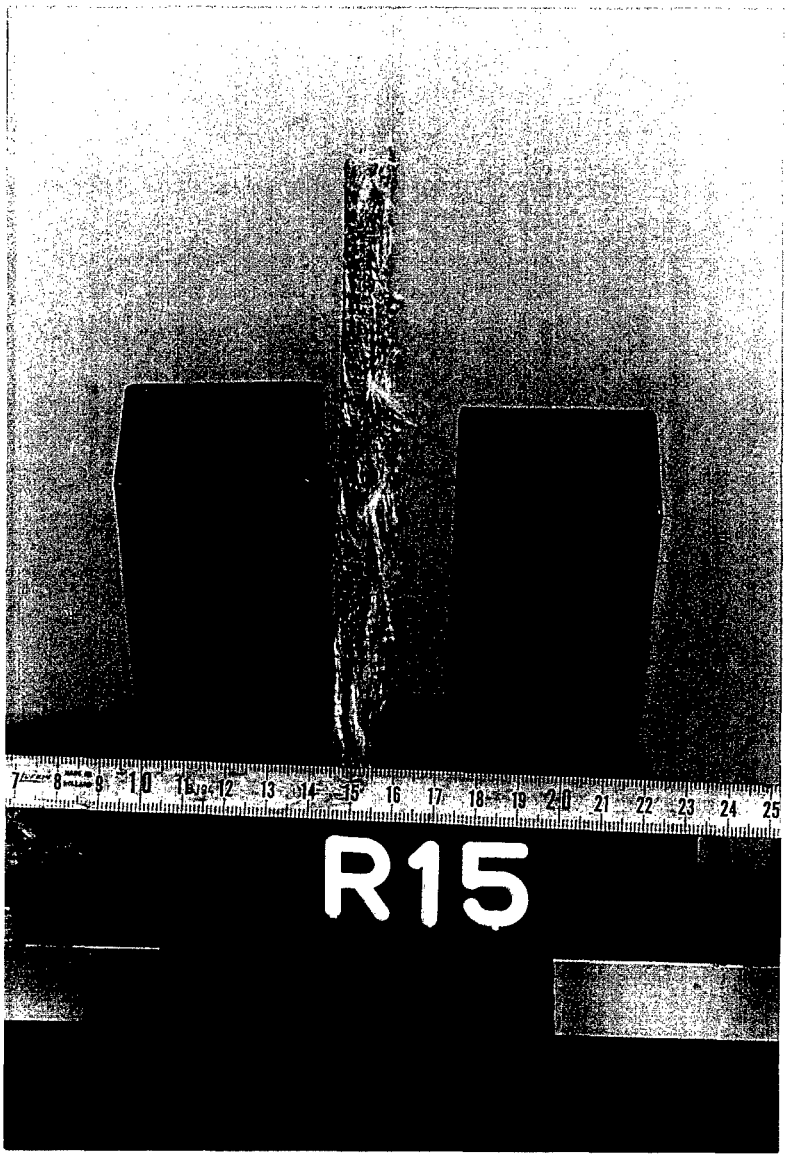

Figure 5: The post-impacted KFRP target from the side impacted with a 2.8 g FSP at 511 m/s (exp. no. 15) (980816-15A).

4.2 Experiments with the GFRP panels

The measured data of all the experiments with the GFRP panels are shown in Annex C. The experiments with the blunt nose (tip angle 120°) projectile were successful and provided suitable data to verify computer simulation models. The experiments with the sharp nose (37°) projectiles, however, were unusable for analysis, because in almost every experiment the projectile deflected from its trajectory (i.e. the line of fire) within the target while penetrating. This can be clearly seen in Figures 6.a and 6.b, which show the IMAX frame sequence of experiment no. 30 and the post-impacted specimen of experiment no. 36 from the side, respectively.

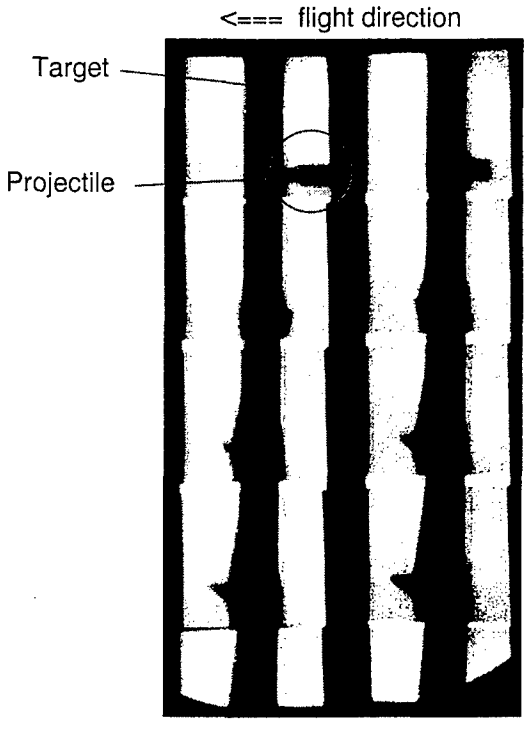

Figure 6.a: IMAX frame sequence of sharp nose FSP impacting GFRP target (exp. no. 30)

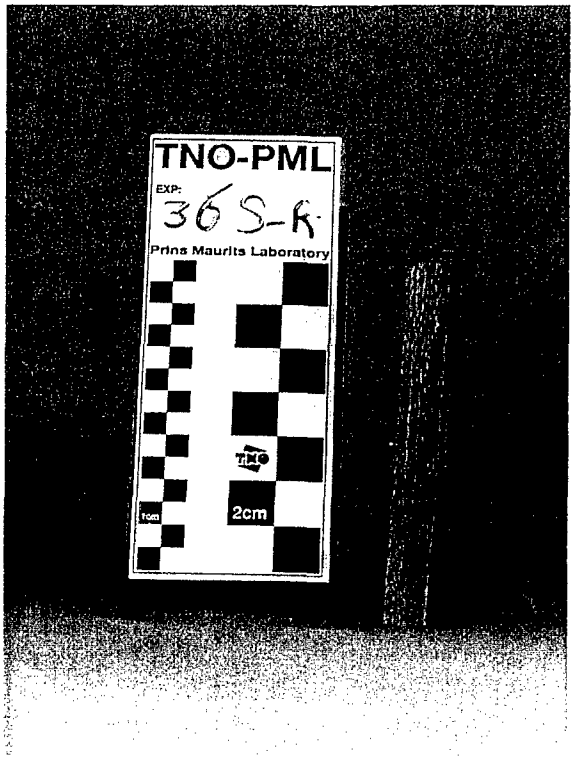

Figure 6.b: The post-impacted GFRP panel from the side after impact with a sharp nose FSP (exp. no. 36) (980814-28).

The IMAX frame sequence (Figure 6.a) shows that the projectile impacts the target with no significant yaw. However, after impact, the projectile starts to deflect from a straight trajectory, which can be seen as the pointed nose of the protectile comes out obliquely at the back of the target.
To examine this phenomena, the flight characteristics of this projectile were simulated with our flight ballistic program 6 Dimension of Flight (6 DOF) of WB2d/Phantom III. These show that the projectile had no pitch and yaw angle and was dynamically stable. The reason for the deflection is probably because the projectile was not spin stabilised. The projectile will therefore be just as stable as a sphere on a hill. With any disturbance, like impacting a target, the deviation will only increase.

For the GFRP panel experiments it must be realised that the lateral dimensions of the target panels are too small to avoid boundary effects. The delamination area reach the boundaries for all the experiments with the blunt nose projectile. An example is shown in Figure 7, which shows the post-impacted specimen of experiment no. 20 from the side. The behaviour of a larger panel in which the delamination does not reach the boundary will be different. Therefore, no trend for the penetration process in GFRP panels can be observed from these experiments.

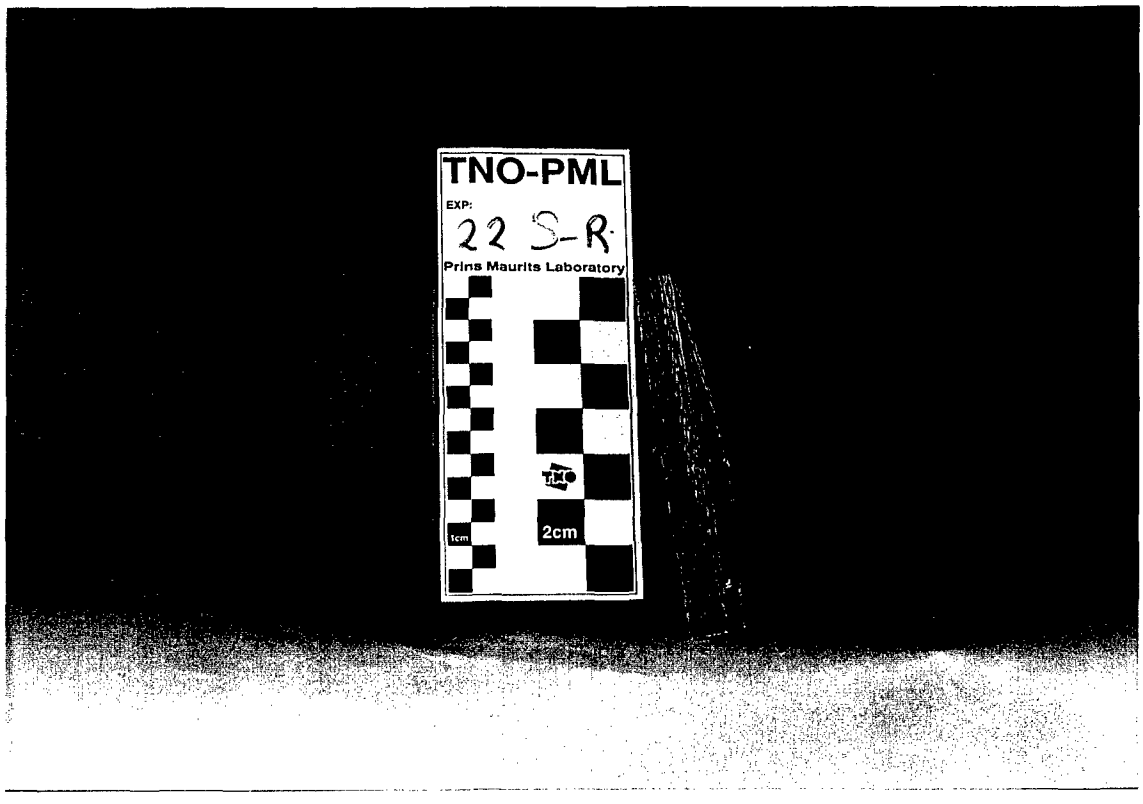

Figure 7: The post-impacted 19 mm thick GFRP target from the side impacted with a blunt nose FSP at 785 m/s (exp. no. 22) (980814-13).

Annex C shows the IMAX and VISAR data measurements graphically. From these data, the following remarkes can be made:

- the backface of the targets reaches its maximum velocity within the first 10 μsec. This velocity change could not be recorded with the VISAR, because the settings were not suitable for measuring such fast velocity changes;
- the displacement profile of the back was measured directly from the IMAX data and indirectly from the velocity profile of the VISAR by integrating the velocity profile;
- the two displacement profiles for the blunt nose projectile experiments correspond reasonably well with each other. However, in some experiments (nos. 16, 20, 22, 23, 24), the VISAR signal was lost after 50 to 80 μsec. So, the VISAR displacement profile is only displayed within this short time-frame;

- the two displacement profiles for the sharp nose projectile experiments do not correspond so well with each other, except for experiment 34. The displacement profile of the VISAR of experiments 30 and 32 correspond with the displacement profile of the projectile measured from the IMAX data. This is due to the fact that the VISAR measuring point was reflected from the projectile when it perforated the target;
- the displacement of the projectile could not be measured in almost any of the experiments. This is due to the fact that the GFRP panels show a large delamination area.

4.3 Modelling results

The UBC is developing an analytical simulation program called IMPACT and a composite failure model for the LS DYNA hydrocode, both for ballistic impact on composite materials under assignment of DREV. In 1996, TNO-PML received the first version of the IMPACT model [1] and the failure model UMAT46V for LSDYNA 2D [2].
Both models have been reviewed, and the IMPACT model version 1.0 has been briefly validated. The results have been reported in a memo to KPU [4].
The IMPACT model was developed in the first place to simulate non-visco-elastic materials, like carbon and glass-fibre reinforced composites, impacted by rigid rod projectiles, like FSPs, at low velocities (<300 m/s). The results in reference 4 show that the model also shows good results for aramide fibre reinforced composites impacted with an FSP at 500-600 m/s.
The failure model UMAT46V could not be validated, because of problems with implementing it. It seems that it cannot be implemented into the hydrocode Autodyn, which is used extensively at TNO-PML. The possibilities in obtaining a code in which it can be implemented, like LSDYNA 2D or MADYMO from TNO-WT, is now under investigation.

5 Conclusions

From the experiments conducted within this project, the following conclusions can be made.

1 The experiments with the KFRP panels were successful and gave very reliable and suitable data to verify computer simulation models.
2 The displacements profiles of the back of the KFRP panels measured with the IMAX and VISAR correspond well with each other.
3 The results of these experiments show the following trend for the penetration process of an FSP impacting a KFRP panel. First the FSP penetrates the fibre reinforced composite by shearing the fibres and pushing the intact material in front, which causes the fibres to stretch. In this phase, a part of the kinetic energy of the projectile is absorbed by the shearing process and strain energy in the fibres. After the shearing process has finished, the straining of the fibres continues until all the kinetic energy is absorbed or until the projectile has completely penetrated the target.
4 The experiments with the GFRP panels with the blunt nose (120°) FSP were successful and gave suitable data to verify computer simulation models.
5 The lateral dimensions of the GFRP panels were too small to avoid boundary effects. The delamination area reaches the boundaries for all the experiments with the blunt nose projectile. The behaviour of a larger panel in which the delamination does not reach the boundary will be different. Therefore no trend for the penetration process in GFRP panels can be observed from these experiments.
6 The experiments with the GFRP panels with the sharp nose (37°) FSP were unusable for analysis, because in almost all experiments the projectile deflected from a straight trajectory through the target. This data is therefore not suitable for verification of the simulation models, because in these models it is assumed that the projectile penetrates the target in a straight line.

6 References

[1] User's Guide,
UBC IMPACT©, Engineering Simulation Sotware, version 1.0,
Composites Group, The University of British Columbia.

[2] Williams, K.V. and Vaziri, R.,
Numerical Study of the Response of Advanced Polymeric Composites to High Velocity Impact, Final report,
Metals and Materials Engineering, Composites Group, UBC, March 1996.

[3] Heiden, N. van der and Bree, J.M.L.J. van,
Evaluation of the behaviour of a copper liner for indentation response analyses in composite helmets under FSP impact,
TNO report PML 1994-A86, April 1995.

[4] Deutekom, M.J.,
Tussenrapportage over het project 'PGU Canadees-Nederlandse samenwerking',
Brief 98D3/1269 aan P. van der Geijs en J.M. de Koning, 3 juni 1998.

7 Authentication

M.J. Deutekom
Project leader/Author

J.L.M.J. van Bree
Research co-ordinator

Dr. H.J. Reitsma
Group leader

Annex A Specimen holder

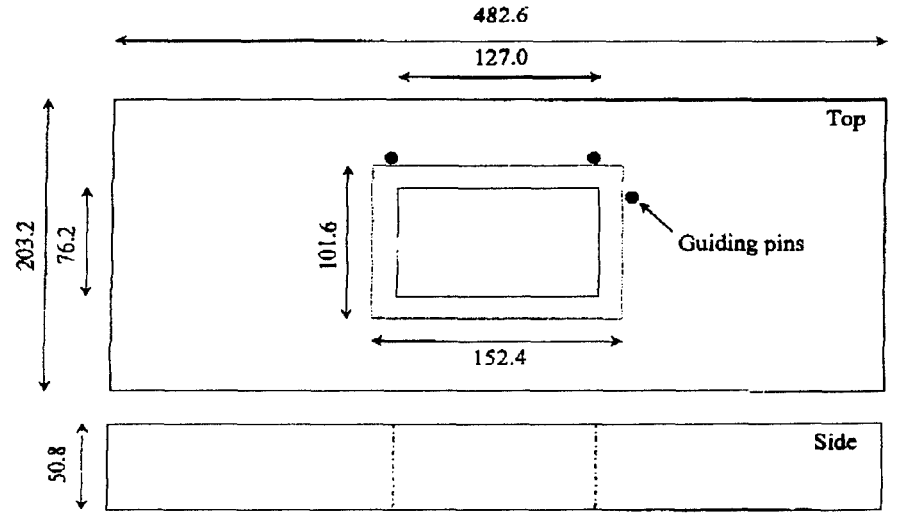

Figure A.1: Schematic drawing of the specimen holder.

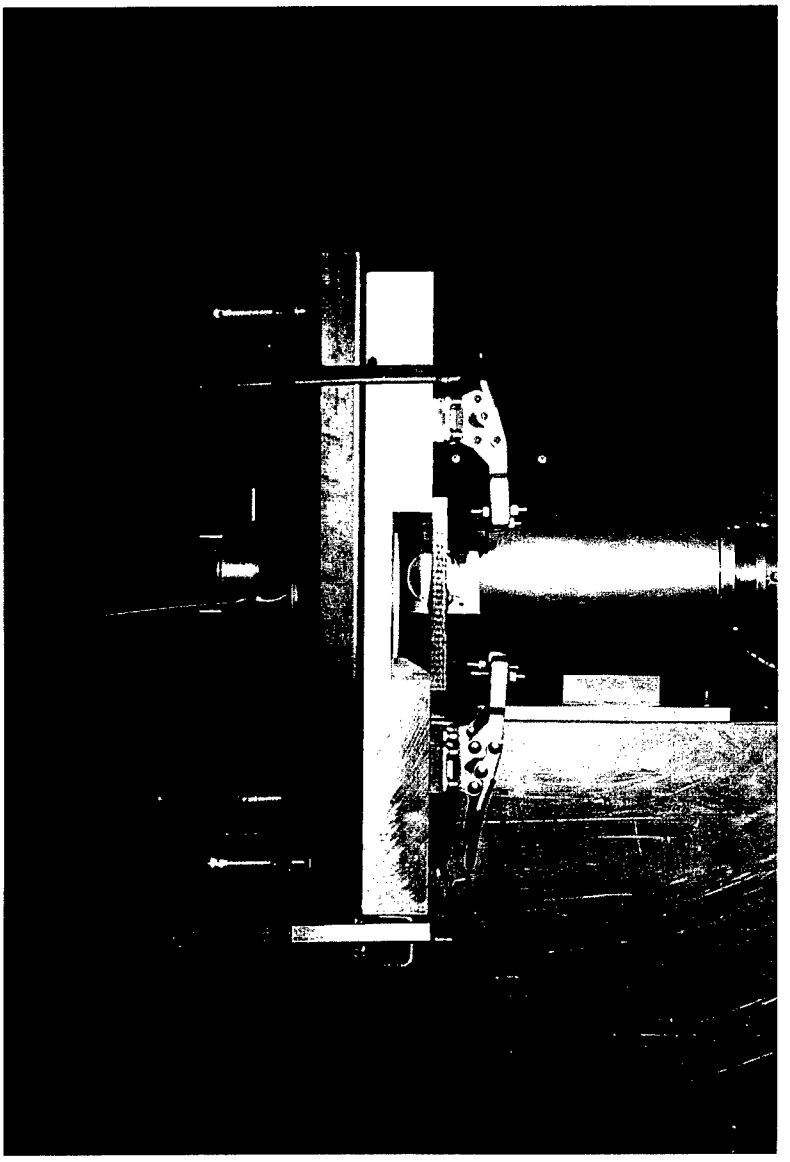

Figure A.2: A picture of the specimen holder from the side where the target is clamped upon (980816-7A).

Annex B Projectile dimensions used for the ballistic impact tests on GFRP panels

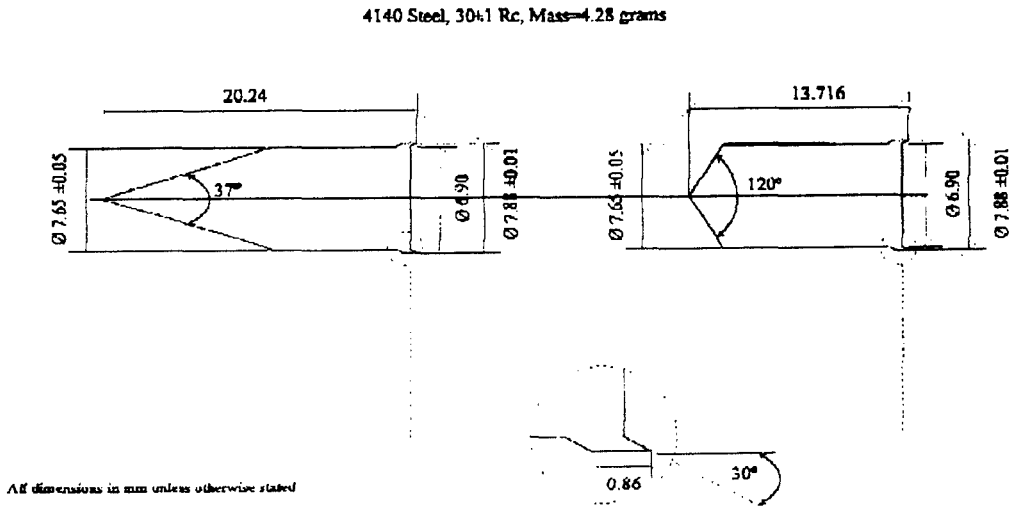

Figure B.1: Projectile dimensions used for the ballistic impact tests on GFRP panels.

Annex C Data impact experiments

Displacement and velocity measurements for the KFRP impact experiments with the 1.1 g FSP.

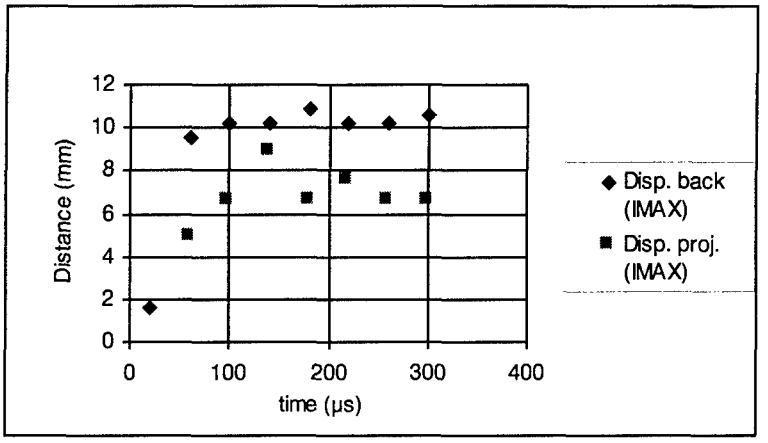

Figure C.1: IMAX and VISAR data for exp. no. 2 (KFRP, 1.1 g FSP, Vin = 588 m/s).

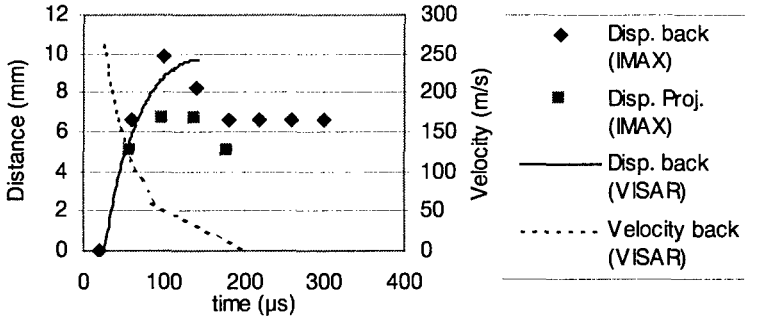

Figure C.2: IMAX and VISAR data for exp. no. 3 (KFRP, 1.1 g FSP, Vin = 586 m/s).

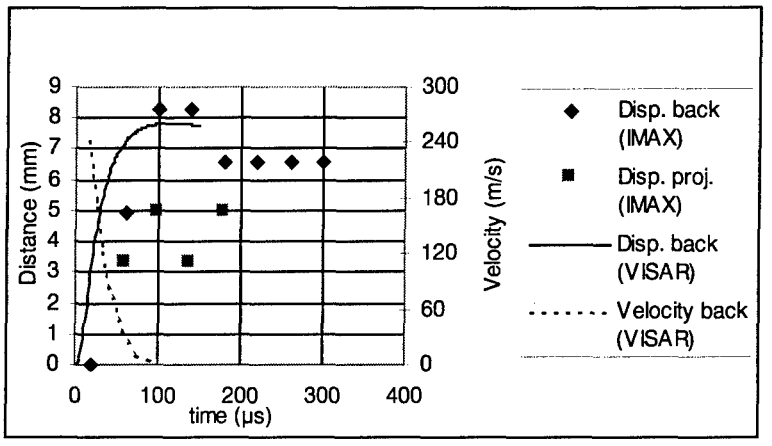

Figure C.3: IMAX and VISAR data for exp. no. 4 (KFRP, 1.1 g FSP, Vin = 560 m/s).

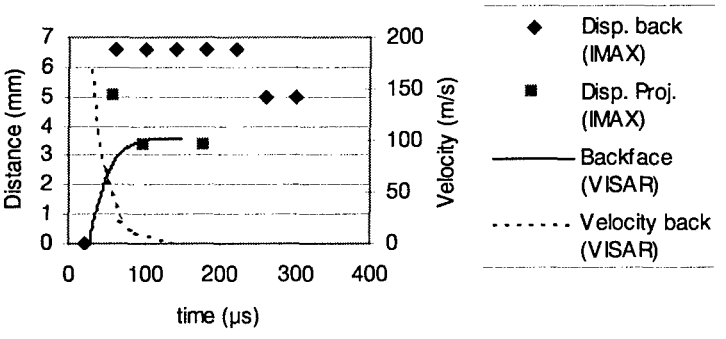

Figure C.4: IMAX and VISAR data for exp. no. 5 (KFRP, 1.1 g FSP, Vin = 564 m/s).

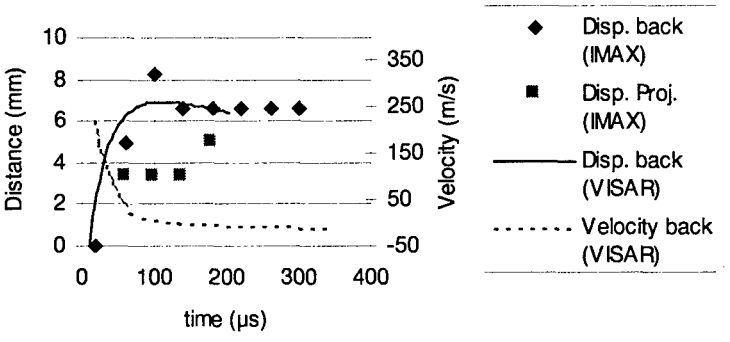

Figure C.5: IMAX and VISAR data for exp. no. 6 (KFRP, 1.1 g FSP, Vin = 545 m/s).

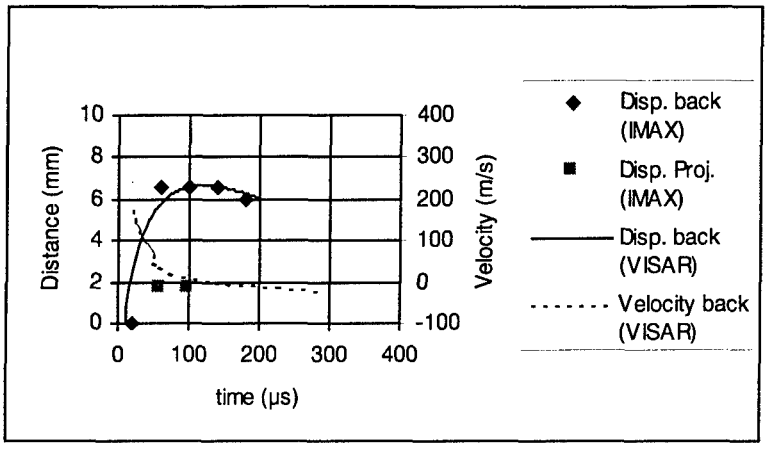

Figure C.6: IMAX and VISAR data for exp. no. 7 (KFRP, 1.1 g FSP, Vin = 483 m/s).

Displacement and velocity measurements for the KFRP impact experiments with the 2.8 g FSP.

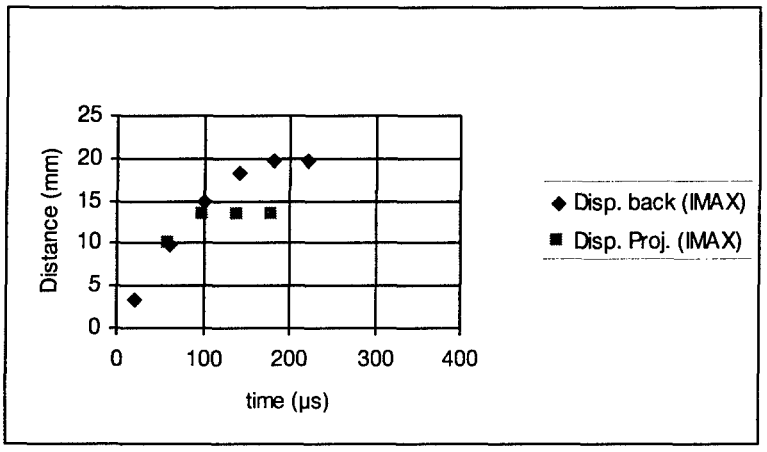

Figure C.7: IMAX and VISAR data for exp. no. 8 (KFRP, 2.8 g FSP, Vin = 490 m/s).

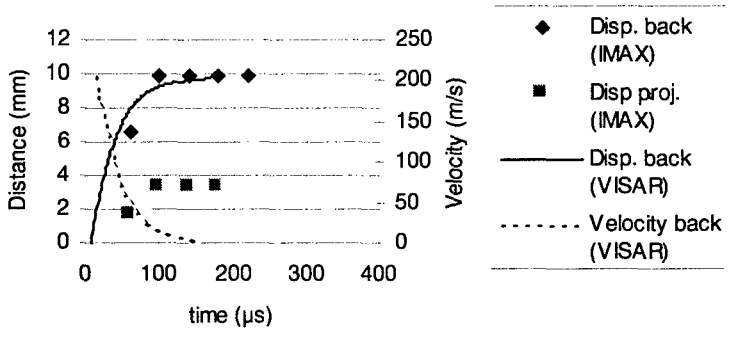

Figure C.8: IMAX and VISAR data for exp. no. 9 (KFRP, 2.8 g FSP, Vin = 398 m/s).

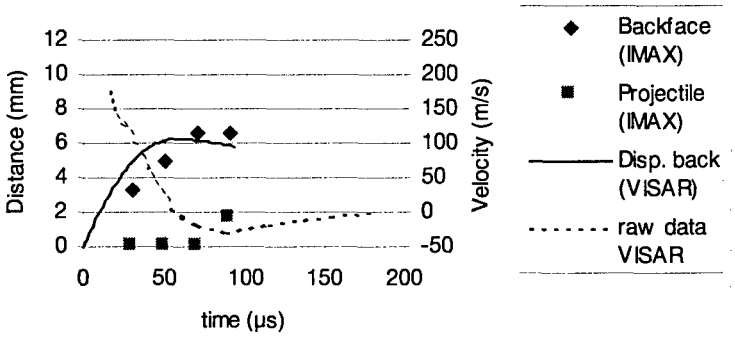

Figure C.9: IMAX and VISAR data for exp. no. 11 (KFRP, 2.8 g FSP, Vin = 386 m/s).

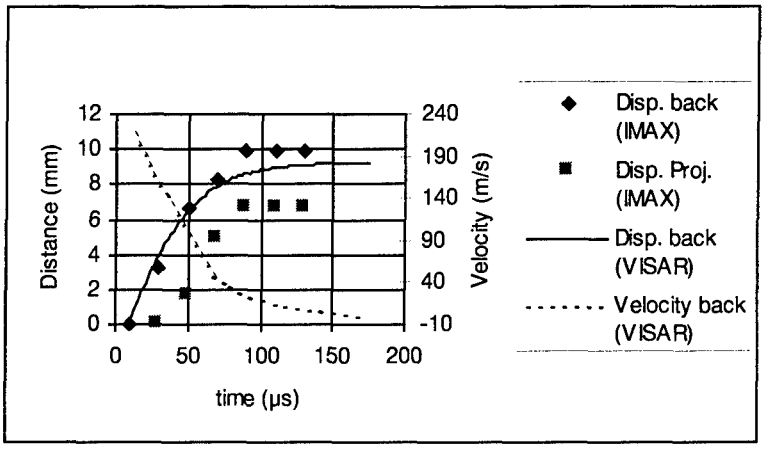

Figure C.10: IMAX and VISAR data for exp. no. 12 (KFRP, 2.8 g FSP, Vin = 446 m/s).

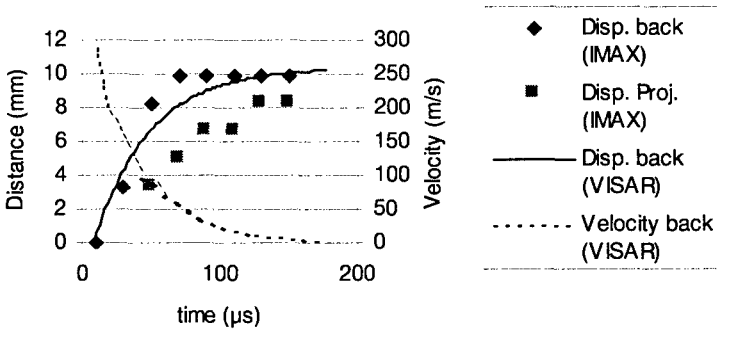

Figure C.11: IMAX and VISAR data for exp. no. 13 (KFRP, 2.8 g FSP, Vin = 461 m/s).

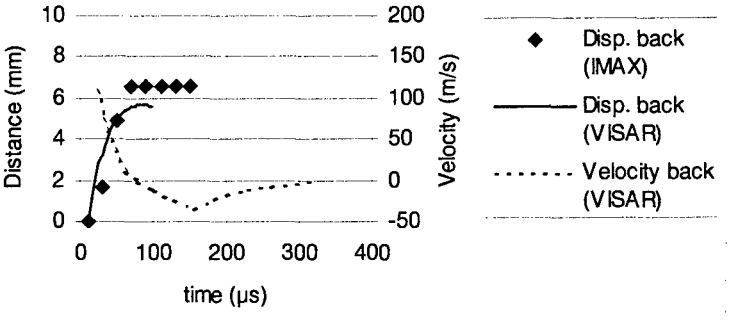

Figure C.12: IMAX and VISAR data for exp. no. 14 (KFRP, 2.8 g FSP, Vin = 321 m/s).

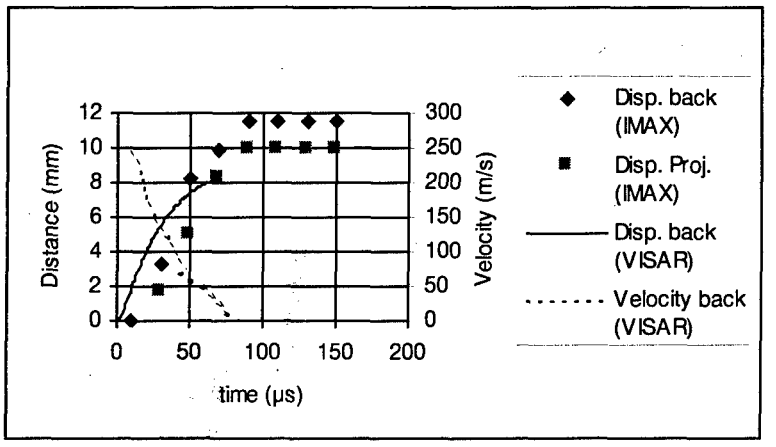

Figure C.13: IMAX and VISAR data for exp. no. 15 (KFRP, 2.8 g FSP, Vin = 511 m/s).

Displacement and velocity measurements for the 12.7 mm thick GFRP impact experiments with the blunt nose (tip angle 120°) FSP.

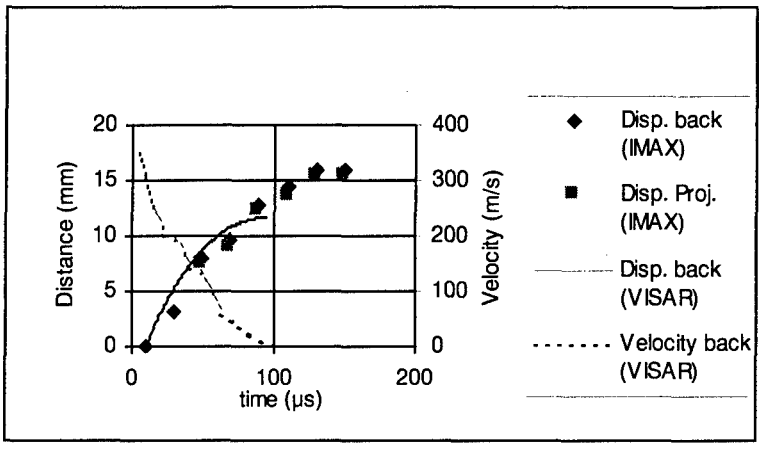

Figure C.14: IMAX and VISAR data for exp. no. 16 (12.7 mm GFRP, 120° FSP, Vin = 557 m/s).

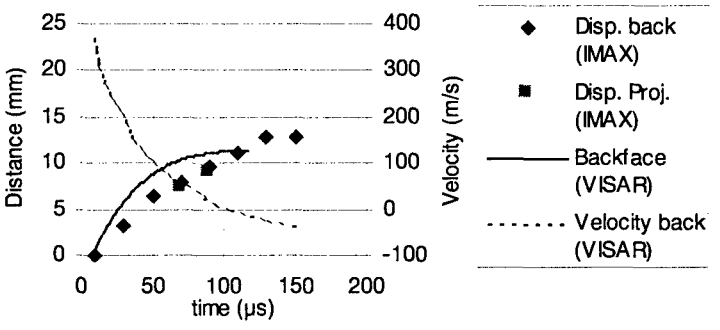

Figure C.15: IMAX and VISAR data for exp. no. 17 (12.7 mmGFRP, 120° FSP, Vin = 517 m/s).

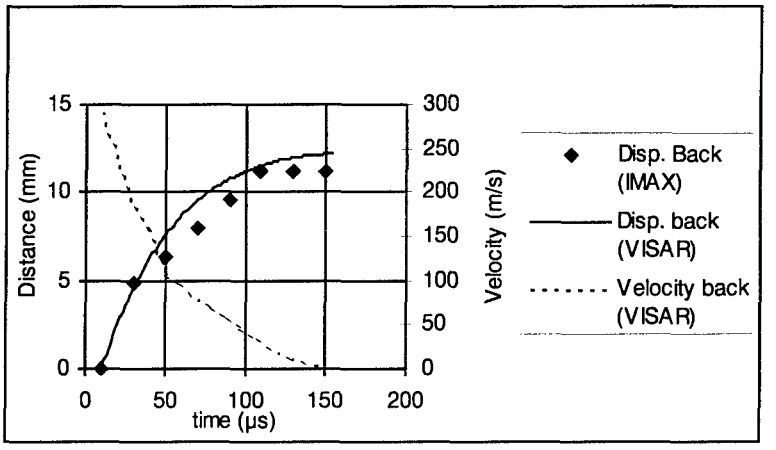

Figure C.16: IMAX and VISAR data for exp. no. 18 (12.7 mm GFRP, 120° FSP, Vin = 526 m/s).

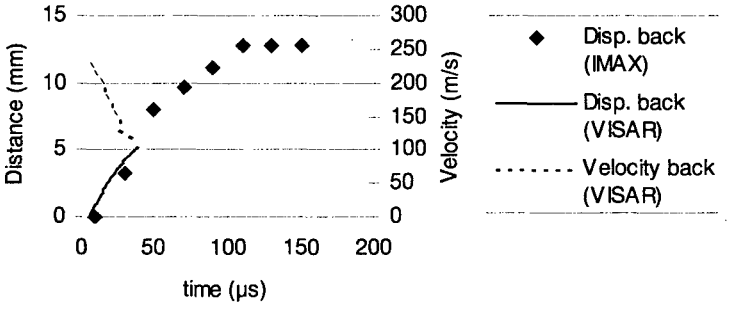

Figure C.17: IMAX and VISAR data for exp. no. 20 (12.7 mm GFRP, 120° FSP, Vin = 548 m/s).

Displacement and velocity measurements for the 19.0 mm thick GFRP impact experiments with the blunt nose (tip angle 120°) FSP.

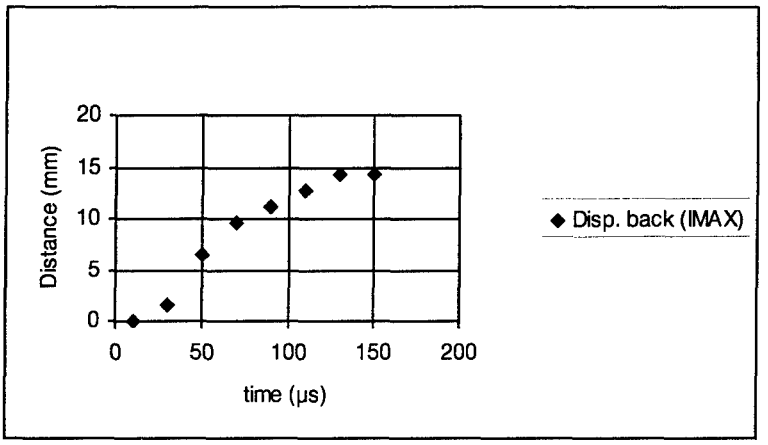

Figure C.18: IMAX and VISAR data for exp. no. 21 (19 mm GFRP, 120° FSP, Vin = 778 m/s).

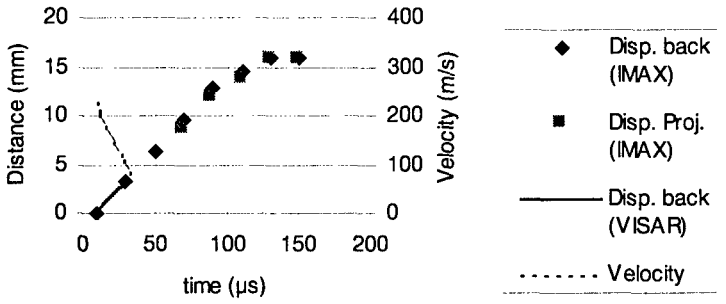

Figure C.19: IMAX and VISAR data for exp. no. 22 (19 mm GFRP, 120° FSP, Vin = 785 m/s).

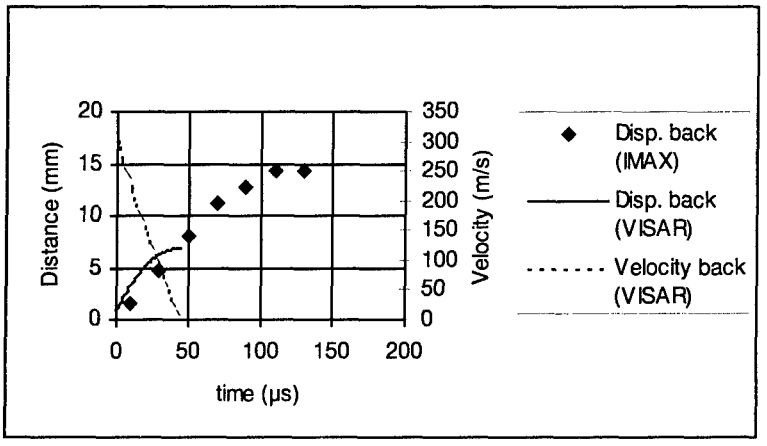

Figure C.20: IMAX and VISAR data for exp. no. 23 (19 mm GFRP, 120° FSP, Vin = 778 m/s).

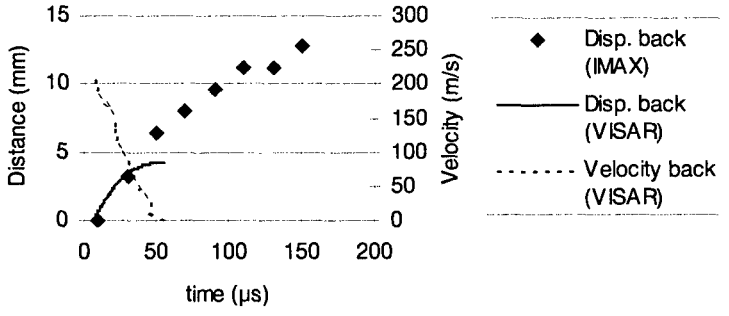

Figure C.21: IMAX and VISAR data for exp. no. 24 (19 mm GFRP, 120° FSP, Vin = 741 m/s).

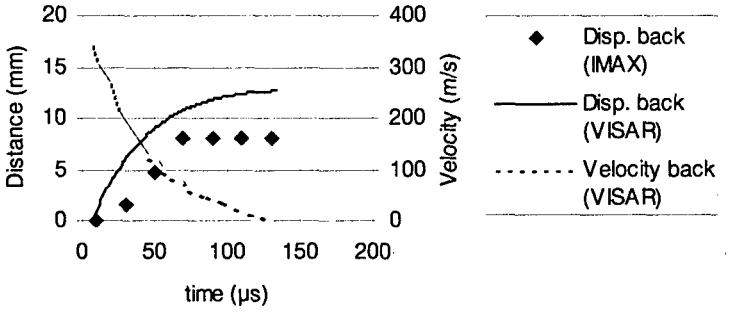

Figure C.22: IMAX and VISAR data for exp. no. 25 (19 mm GFRP, 120° FSP, Vin = 660 m/s).

Displacement and velocity measurements for the 12.7 mm thick GFRP impact experiments with the sharp nose (tip angle 37°) FSP.

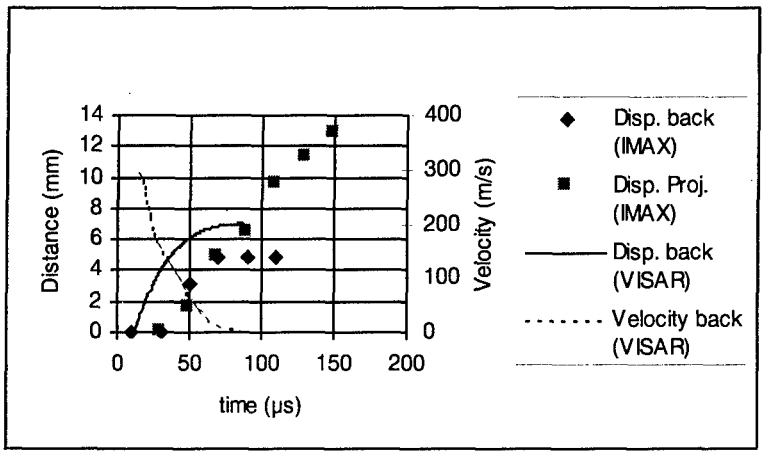

Figure C.23: IMAX and VISAR data for exp. no. 30 (12.7 mm GFRP, 37° FSP, Vin = 388 m/s).

Displacement and velocity measurements for the 19.0 mm thick GFRP impact experiments with the sharp nose (tip angle 37°) FSP.

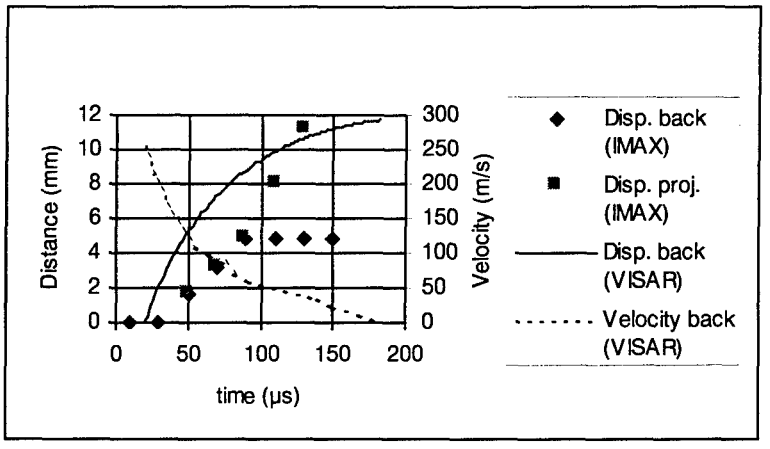

Figure C.24: IMAX and VISAR data for exp. no. 32 (19 mm GFRP, 37° FSP, Vin = 466 m/s).

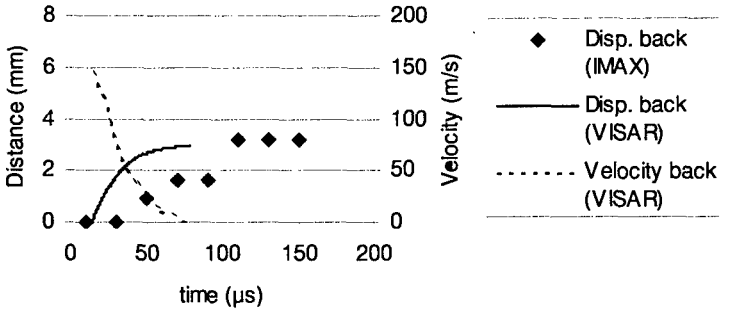

Figure C.25: IMAX and VISAR data for exp. no. 34 (19 mm GFRP, 37° FSP, Vin = 420 m/s).

REPORT DOCUMENTATION PAGE
(MOD-NL)

1. DEFENCE REPORT NO. (MOD-NL)	2. RECIPIENT'S ACCESSION NO.	3. PERFORMING ORGANIZATION REPORT NO.
TD98-0347		PML 1998-A106
4. PROJECT/TASK/WORK UNIT NO.	**5. CONTRACT NO.**	**6. REPORT DATE**
231096210	A96KL453	March 1999
7. NUMBER OF PAGES	**8. NUMBER OF REFERENCES**	**9. TYPE OF REPORT AND DATES COVERED**
39 (incl. 3 annexes, excl. RDP & distribution list)	4	Final

10. TITLE AND SUBTITLE

Evaluation of the ballistic resistance of composite materials under FSP impact: experimental results

11. AUTHOR(S)

M.J. Deutekom

12. PERFORMING ORGANIZATION NAME(S) AND ADDRESS(ES)

TNO Prins Maurits Laboratory, P.O. Box 45, 2280 AA Rijswijk, The Netherlands
Lange Kleiweg 137, Rijswijk, The Netherlands

13. SPONSORING AGENCY NAME(S) AND ADDRESS(ES)

LBBKL-KPU-bedrijf, P.O. Box 3003, 3800 DA Amersfoort, The Netherlands

14. SUPPLEMENTARY NOTES

The classification designation Ongerubriceerd is equivalent to Unclassified.

15. ABSTRACT (MAXIMUM 200 WORDS (1044 BYTE))

Personal protection equipment of the soldier consists more and more of polymeric composite materials. To understand the ballistic resistance of these materials, a reliable analysis tool is necessary. However, there is still a need for reliable experimental data to calibrate and validate the simulation predictions.
The University of British Columbia (UBC) in Vancouver is developing simulation models for ballistic impact on composite materials under assignment from the Defence Research Establishment Valcartier (DREV). A joint project with DREV was started to study the impact behaviour of fibre reinforced plastics (FRP). To validate the models, TNO Prins Maurits Laboratory (TNO-PML) performed instrumented ballistic impact experiments on two types of FRPs impacted by FSPs (Fragment Simulating Projectiles). A cineradiographic high-speed camera (IMAX) was used to measure the displacement of the backface and FSP during impact. A Velocity Interference System for Any Reflector (VISAR) was also used to measure the velocity changes at the backface of the target. The experiments with the aramide FRP panels were successful and gave very reliable data to verify computer simulation models. A trend for the penetration process could not be observed.

16. DESCRIPTORS

Ballistic protection
Composite materials
Experimentation
FSP projectiles
Military personnel
Protective equipment

17a. SECURITY CLASSIFICATION (OF REPORT)	17b. SECURITY CLASSIFICATION (OF PAGE)	17c. SECURITY CLASSIFICATION (OF ABSTRACT)
Ongerubriceerd	Ongerubriceerd	Ongerubriceerd

18. DISTRIBUTION AVAILABILITY STATEMENT	17d. SECURITY CLASSIFICATION (OF TITLES)
Unlimited Distribution	Ongerubriceerd

Distributielijst*

1	DWOO
2	HWO-KL
3*	HWO-KLu
4*	HWO-KM
5*	HWO-CO
6	LBBKL-KPU-bedrijf, Hoofd BBV C.M.C.M. Schakenraad
7/8	LBBKL-KPU-bedrijf, BBV, Hoofd Sie Onderzoek & Ontwikkeling Ing. J.M. de Koning
9	DM&P TNO-DO
10*	DM&P TNO-DO, accountcoördinator KL
11*	TNO-FEL, Bibliotheek
12/14	Bibliotheek KMA
15*	Lid Instituuts Advies Raad PML BGen. Prof. J.M.J. Bosch
16*	Lid Instituuts Advies Raad PML Ir. A.H.P.M. Schaeken
17*	Lid Instituuts Advies Raad PML Prof. ir. J.A. Schot
18*	Lid Instituuts Advies Raad PML Prof. ir. K.F. Wakker
19	TNO-PML, Directie; daarna reserve
20	TNO-PML, Hoofd Divisie Wapens en Wapenplatformen Dr. D.W. Hoffmans
21/23	TNO-PML, Divisie Wapens en Wapenplatformen Dr. H.J. Reitsma, Ir. J.L.M.J. van Bree en Ir. M.J. Deutekom
24	TNO-PML, Documentatie
25	TNO-PML, Archief

* De met een asterisk (*) gemerkte instanties/personen ontvangen uitsluitend de titelpagina, het managementuittreksel, de documentatiepagina en de distributielijst van het rapport.